

---

# Open-YOLO 3D: Towards Fast and Accurate Open-Vocabulary 3D Instance Segmentation

---

Mohamed El Amine Boudjoghra<sup>1</sup>, Angela Dai<sup>2</sup>, Jean Lahoud<sup>1</sup>,  
Hisham Cholakkal<sup>1</sup>, Rao Muhammad Anwer<sup>1,3</sup>, Salman Khan<sup>1,4</sup>, Fahad Shahbaz Khan<sup>1,4</sup>

<sup>1</sup>Mohamed Bin Zayed University of Artificial Intelligence (MBZUAI),

<sup>2</sup>Technical University of Munich (TUM), <sup>3</sup>Aalto University,

<sup>4</sup>Australian National University, <sup>5</sup>Linköping University

{mohamed.boudjoghra, jean.lahoud, hisham.cholakkal,  
rao.anwer, salman.khan, fahad.khan}@mbzuai.ac.ae, angela.dai@tum.de

## Abstract

Recent works on open-vocabulary 3D instance segmentation show strong promise, but at the cost of slow inference speed and high computation requirements. This high computation cost is typically due to their heavy reliance on 3D clip features, which require computationally expensive 2D foundation models like Segment Anything (SAM) and CLIP for multi-view aggregation into 3D. As a consequence, this hampers their applicability in many real-world applications that require both fast and accurate predictions. To this end, we propose a fast yet accurate open-vocabulary 3D instance segmentation approach, named Open-YOLO 3D, that effectively leverages only 2D object detection from multi-view RGB images for open-vocabulary 3D instance segmentation. We address this task by generating class-agnostic 3D masks for objects in the scene and associating them with text prompts. We observe that the projection of class-agnostic 3D point cloud instances already holds instance information; thus, using SAM might only result in redundancy that unnecessarily increases the inference time. We empirically find that a better performance of matching text prompts to 3D masks can be achieved in a faster fashion with a 2D object detector. We validate our Open-YOLO 3D on two benchmarks, ScanNet200 and Replica, under two scenarios: (i) with ground truth masks, where labels are required for given object proposals, and (ii) with class-agnostic 3D proposals generated from a 3D proposal network. Our Open-YOLO 3D achieves state-of-the-art performance on both datasets while obtaining up to  $\sim 16\times$  speedup compared to the best existing method in literature. On ScanNet200 val. set, our Open-YOLO 3D achieves mean average precision (mAP) of 24.7% while operating at 22 seconds per scene. Code and model are available at [github.com/aminebdj/OpenYOLO3D](https://github.com/aminebdj/OpenYOLO3D)

## 1 Introduction

3D instance segmentation is a computer vision task that involves the prediction of masks for individual objects in a 3D point cloud scene. It holds significant importance in fields like robotics and augmented reality. Due to its diverse applications, this task has garnered increasing attention in recent years. Researchers have long focused on methods that typically operate within a closed-set framework, limiting their ability to recognize objects not present in the training data. This constraint poses challenges, particularly when novel objects must be identified or categorized in unfamiliar environments. Recent methods [34, 42] address the problem of novel class segmentation, but they suffer from slow inference that ranges from 5 minutes for small scenes to 10 minutes for large scenes

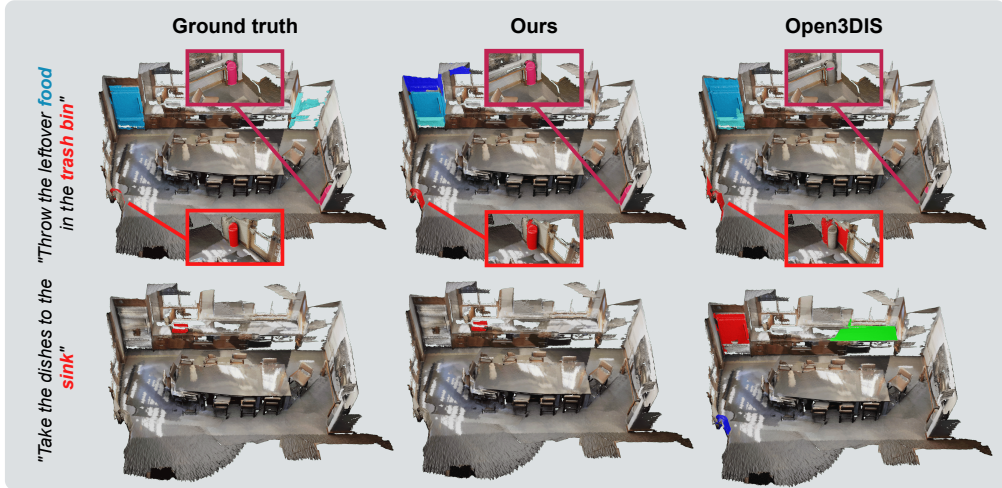


Figure 1: **Open-vocabulary 3D instance segmentation with our Open-YOLO 3D.** The proposed Open-YOLO 3D is capable of segmenting objects in a zero-shot manner. Here, We show the output for a ScanNet200 [38] scene with various prompts, where our model yields improved performance compared to the recent Open3DIS [34]. We show zoomed-in images of hidden predicted instances in the colored boxes. Additional results are in Figure 4 and suppl. material.

due to their reliance on computationally heavy foundation models like SAM [23] and CLIP [55] along with heavy computation for lifting 2D CLIP feature to 3D.

Open-vocabulary 3D instance segmentation is important for robotics tasks such as, material handling where the robot is expected to perform operations from text-based instructions like moving specific products, loading and unloading goods, and inventory management while being fast in the decision-making process. Although state-of-the-art open-vocabulary 3D instance segmentation methods show high promise in terms of generalizability to novel objects, they still operate in minutes of inference time due to their reliance on heavy foundation models such as SAM. Motivated by recent advances in 2D object detection [7], we look into an alternative approach that leverages fast object detectors instead of utilizing computationally expensive foundation models.

This paper proposes a novel open-vocabulary 3D instance segmentation method, named Open-YOLO 3D, that utilizes efficient, joint 2D-3D reasoning, using 2D bounding box predictions to replace computationally-heavy segmentation models. We employ an open-vocabulary 2D object detector to generate bounding boxes with their class labels for all frames corresponding to the 3D scene; on the other side, we utilize a 3D instance segmentation network to generate 3D class-agnostic instance masks for the point clouds, which proves to be much faster than 3D proposal generation methods from 2D instances [34, 32]. Unlike recent methods [42, 34] which use SAM and CLIP to lift 2D clip features to 3D for prompting the 3D mask proposal, we propose an alternative approach that relies on the bounding box predictions from 2D object detectors which prove to be significantly faster than CLIP-based methods. We utilize the predicted bounding boxes in all RGB frames corresponding to the point cloud scene to construct a Low Granularity (LG) label map for every frame. One LG label map is a two-dimensional array with the same height and width as the RGB frame, with the bounding box areas replaced by their predicted class label. Next, we use intrinsic and extrinsic parameters to project the point cloud scene onto their respective LG label maps with top-k visibility for final class prediction. We present an example output of our method in Figure 1. Our contributions are following:

- We introduce a 2D object detection-based approach for open-vocabulary labeling of 3D instances, which greatly improves the efficiency compared to 2D segmentation approaches.
- We propose a novel approach to scoring 3D mask proposals using only bounding boxes from 2D object detectors.
- Our Open-YOLO 3D achieves superior performance on two benchmarks, while being considerably faster than existing methods in the literature. On ScanNet200 val. set, our Open-YOLO 3D achieves an absolute gain of 2.3% at mAP50 while being  $\sim 16x$  faster compared to the recent Open3DIS [34].

## 2 Related works

**Closed-vocabulary 3D segmentation:** The 3D instance segmentation task aims at predicting masks for individual objects in a 3D scene, along with a class label belonging to the set of known classes. Some methods use a grouping-based approach in a bottom-up manner, by learning embeddings in the latent space to facilitate clustering of object points [4, 14, 15, 21, 26, 29, 46, 54]. Conversely, proposal-based methods adopt a top-down strategy, initially detecting 3D bounding boxes and then segmenting the object region within each box [10, 17, 31, 49, 52]. Notably, inspired by advancements in 2D works [5, 6], transformer designs [43] have been recently applied to 3D instance segmentation tasks [39, 41, 24, 1, 20]. Mask3D [39] introduces the first hybrid architecture that combines Convolutional Neural Networks (CNN) and transformers for this task. It uses a 3D CNN backbone to extract per-point features and a transformer-based instance mask decoder to refine a set of queries. Building on Mask3D, the authors of [1] show that using explicit spatial and semantic supervision at the level of the 3D backbone further improves the instance segmentation results. Oneformer3D [24] follows a similar architecture and introduces learnable kernels in the transformer decoder for a unified semantic, instance, and panoptic segmentation. ODIN [20] proposes an architecture that uses 2D-3D fusion to generate the masks and class labels. Other methods introduce weakly-supervised alternatives to dense annotation approaches, aiming to reduce the annotation cost associated with 3D data [8, 18, 47]. While these methodologies strive to enhance the quality of 3D instance segmentation, they typically rely on a predefined set of semantic labels. In contrast, our proposed approach aims at segmenting objects with both known and unknown class labels.

**Open-vocabulary 2D recognition:** This task aims at identifying both known and novel classes, where the labels of the known classes are available in the training set, while the novel classes are not encountered during training. In the direction of open-vocabulary object detection (OVOD), several approaches have been proposed [58, 36, 30, 53, 45, 22, 51, 7]. Another widely studied task is open-vocabulary segmentation (OVSS) [3, 48, 27, 12, 28]. Recent open-vocabulary semantic segmentation methods [27, 12, 28] leverage pre-trained CLIP [55] to perform open-vocabulary segmentation, where the model is trained to output a pixel-wise feature that is aligned with the text embedding in the CLIP space. Furthermore, AttrSeg [33] proposes a decomposition-aggregation framework where vanilla class names are first decomposed into various attribute descriptions, and then different attribute representations are aggregated into a final class representation. Open-vocabulary instance segmentation (OVIS) aims at predicting instance masks while preserving high zero-shot capabilities. One approach [19] proposes a cross-modal pseudo-labeling framework, where a student model is supervised with pseudo-labels for the novel classes from a teacher model. Another approach [44] proposes an annotation-free method where a pre-trained vision-language model is used to produce annotations at both the box and pixel levels. Although these methods show high zero-shot performance and real-time speed, they are still limited to 2D applications only.

**Open-vocabulary 3D segmentation:** Several methods [35, 13, 16] have been proposed to address the challenges of open-vocabulary semantic segmentation where they use foundation models like clip for unknown class discovery, while the authors of [2] focus on weak supervision for unknown class discovery without relying on any 2D foundation model. OpenScene [35] makes use of 2D open-vocabulary semantic segmentation models to lift the pixel-wise 2D CLIP features into the 3D space, which allows the 3D model to perform 3D open-vocabulary point cloud semantic segmentation. On the other hand, ConceptGraphs [13] relies on creating an open-vocabulary scene graph that captures object properties such as spatial location, enabling a wide range of downstream tasks including segmentation, object grounding, navigation, manipulation, localization, and remapping. In the direction of 3D point cloud instance segmentation, OpenMask3D [42] uses a 3D instance segmentation network to generate class-agnostic mask proposals, along with SAM [23] and CLIP [55], to construct a 3D clip feature for each mask using RGB-D images associated with the 3D scene. Unlike OpenMask3D where a 3D proposal network is used, OVIR-3D [32] generates 3D proposals by fusing 2D masks obtained by a 2D instance segmentation model. Open3DIS [34] combines proposals from 2D and 3D with novel 2D masks fusion approaches via hierarchical agglomerative clustering, and also proposes to use point-wise 3D CLIP features instead of mask-wise features. The two most recent approaches in [34, 42] show promising generalizability in terms of novel class discovery [42] and novel object geometries especially small objects [34]. However, they both suffer from slow inference speed, as they rely on SAM for 3D mask proposal clip feature aggregation in the case of OpenMask3D [42], and for novel 3D proposal masks generation from 2D masks [34].

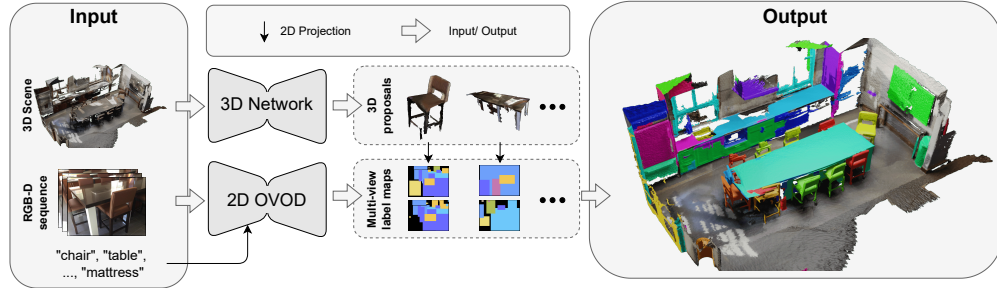


Figure 2: **Proposed open-world 3D instance segmentation pipeline.** We use a 3D instance segmentation network (3D Network) for generating class-agnostic proposals. For open-vocabulary prediction, a 2D Open-Vocabulary Object Detector (2D OVOD) generates bounding boxes with class labels. These predictions are used to construct label maps for all input frames. Next, we assign the top-k label maps to each 3D proposal based on visibility. Finally, we generate a Multi-View Prompt Distribution from the 2D projections of the proposals to match a text prompt to every 3D proposal.

### 3 Preliminaries

**Problem formulation:** 3D instance segmentation aims at segmenting individual objects within a 3D scene and assigning one class label to each segmented object. In the open-vocabulary (OV) setting, the class label can belong to previously known classes in the training set as well as new class labels. To this end, let  $P$  denote a 3D reconstructed point cloud scene, where a sequence of RGB-D images was used for the reconstruction. We denote the RGB image frames as  $\mathcal{I}$  along with their corresponding depth frames  $D$ . Similar to recent methods [35, 42, 34], we assume that the poses and camera parameters are available for the input 3D scene.

#### 3.1 Baseline Open-Vocabulary 3D Instance Segmentation

We base our approach on OpenMask3D [42], which is the first method that performs open-vocabulary 3D instance segmentation in a zero-shot manner. OpenMask3D has two main modules: a class-agnostic mask proposal head, and a mask-feature computation module. The class-agnostic mask proposal head uses a transformer-based pre-trained 3D instance segmentation model [39] to predict a binary mask for each object in the point cloud. The mask-feature computation module first generates 2D segmentation masks by projecting 3D masks into views in which the 3D instances are highly visible, and refines them using the SAM [23] model. A pre-trained CLIP vision-language model [55] is then used to generate image embeddings for the 2D segmentation masks. The embeddings are then aggregated across all the 2D frames to generate a 3D mask-feature representation.

**Limitations:** OpenMask3D makes use of the advancements in 2D segmentation (SAM) and vision-language models (CLIP) to generate and aggregate 2D feature representations, enabling the querying of instances according to open-vocabulary concepts. However, this approach suffers from a high computation burden leading to slow inference times, with a processing time of 5-10 minutes per scene. The computation burden mainly originates from two sub-tasks: the 2D segmentation of the large number of objects from the various 2D views, and the 3D feature aggregation based on the object visibility. We next introduce our proposed method which aims at reducing the computation burden and improving the task accuracy.

## 4 Method: Open-YOLO 3D

**Motivation:** We here present our proposed 3D open-vocabulary instance segmentation method, Open-YOLO 3D, which aims at generating 3D instance predictions in an efficient strategy. Our proposed method introduces efficient and improved modules at the task level as well as the data level. *Task Level:* Unlike OpenMask3D, which generates segmentations of the projected 3D masks, we pursue a more efficient approach by relying on 2D object detection. Since the end target is to generate labels for the 3D masks, the increased computation from the 2D segmentation task is not necessary. *Data Level:* OpenMask3D computes the 3D mask visibility in 2D frames by iteratively counting

visible points for each mask across all frames. This approach is time-consuming, and we propose an alternative approach to compute the 3D mask visibility within all frames at once.

#### 4.1 Overall Architecture

Our proposed pipeline is shown in Figure 2. First, we generate a set of instance proposals  $M$  using a 3D instance segmentation network; the proposals are represented as binary masks, where every 3D mask has a dimension equal to the number of points as the input point cloud. For the open vocabulary prediction, we use a 2D open-vocabulary object detection model to generate a set of bounding boxes denoted  $B_i$  for every frame  $\mathcal{I}_i$ ; the bounding boxes with their predicted labels are used to construct a low-granularity label map  $\mathcal{L}_i$  for every input frame  $\mathcal{I}_i$ . To assign a prompt ID to the 3D mask proposals, we first start by projecting all  $N$  points in the point cloud scene  $P$  onto the  $N_f$  frames, which results in  $N_f$  2D projection with  $N$  points for each. Afterward, the 2D projections and the 3D mask proposals are used to compute the visibility of every mask in every frame using our proposed accelerated visibility computation (**VAcc**); the visibility is then used to assign top-k Low-Granularity label maps to each mask and to select the top-k 2D projections corresponding to every 3D mask proposal; for a single 3D mask we crop the  $(x, y)$  coordinates from the projections using the instance mask and filter out the points that are occluded or outside the frame. The final cropped  $(x, y)$  coordinates from the top-k frames are used to select per-point labels from their corresponding Low-Granularity label maps to finally construct a Multi-View Prompt Distribution to predict the prompt ID corresponding to the 3D mask proposal.

#### 4.2 3D Object Proposal

To generate class-agnostic 3D object proposals, we rely on the 3D instance generation approach Mask3D [39], which allows for faster proposal generation compared to 2D mask-based 3D proposal generation methods [34, 32]. Mask3D is a hybrid model that combines a 3D Convolutional Neural Network as a backbone for feature generation and a transformer-based model for mask instance prediction. The 3D CNN backbone takes the voxelized input point cloud scene as input, and outputs multi-level feature maps, while the transformer decoder takes the multi-level feature maps to refine a set of queries through self and cross-attention. The final refined queries are used to predict instance masks. The 3D proposal network predicts a set  $K_{3D} \in \mathbb{N}$  of 3D mask proposals  $M \in \mathbb{Z}_2^{K_{3D} \times N}$  for a given point cloud  $P \in \mathbb{R}^{4 \times N}$  with  $N$  points in homogeneous coordinate system, where  $\mathbb{Z}_2 = \{0, 1\}$ .

#### 4.3 Low Granularity (LG) Label-Maps

As discussed earlier, the focus of our approach is to generate fast and accurate open-vocabulary labels for the generated 3D proposals. Instead of relying on computationally intensive 2D segmentation, we propose a 2D detection-based approach in our pipeline. For every RGB image  $\mathcal{I}_i$  we generate a set of  $K_{b,i}$  bounding boxes  $B_i = \{(b_j, c_j) \mid b_j \in \mathbb{R}^4, c_j \in \mathbb{N}, \forall j \in (1, \dots, K_{b,i})\}$  using an open-vocabulary 2D object detector, where  $b_j$  are the bounding boxes coordinates while  $c_j$  is its predicted label. We assign a weight  $w_j = b_j^H + b_j^W$  for each output bounding box  $b_j$ , where  $b_j^H$  and  $b_j^W$  are the bounding box’s height and width, respectively. The weights represent the bounding box size and help determine the order of bounding boxes when used to construct the LG label maps.

After obtaining the 2D object detections, we represent the output of each 2D image frame  $\mathcal{I}_i$  as an LG label map  $\mathcal{L}_i \in \mathbb{Z}^{W \times H}$ . To construct  $\mathcal{L}_i$ , we start by initializing all of its elements as **-1**. In our notation, **-1** represents no class and is ignored during prediction. Next, we sort all bounding boxes following their weights and replace the region of the bounding box  $b_j$  with its corresponding predicted class label  $c_j$  in the label map, starting with the bounding box with the highest weight. The weight  $w_j$  choice is motivated by the fact that if two objects of different sizes appear in the same direction the camera is pointing to, the small object is visible in the image if it is closer to the camera than the large object.

#### 4.4 Accelerated Visibility Computation (VAcc)

In order to associate 2D label maps with 3D proposals, we compute the visibility of each 3D mask. To this end, we propose a fast approach that is able to compute 3D mask visibility within frames via tensor operations which are highly parallelizable.

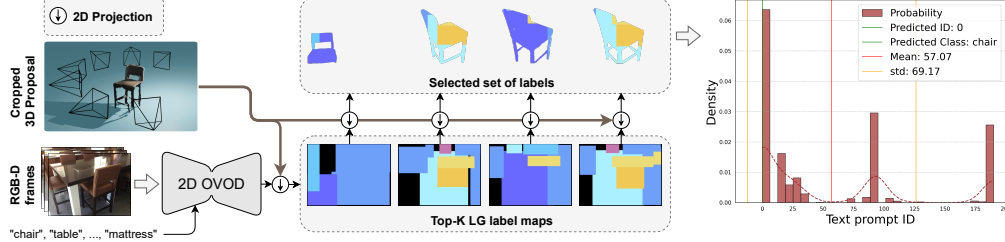


Figure 3: **Multi-View Prompt Distribution (MVPDist)**. After creating the LG label maps for all frames, we select the top-k label maps based on the 2D projection of the 3D proposal. Using the  $(x, y)$  coordinates of the 2D projection, we choose the labels from the LG label maps to generate the MVPDist. This distribution predicts the ID of the text prompt with the highest probability.

Given  $K_f \in \mathbb{N}$  2D RGB frames  $\mathcal{I} = \{\mathcal{I}_i \in \mathbb{R}^{3 \times W \times H} \mid \forall i \in (1, \dots, K_f)\}$  associated with the 3D scene  $P$ , along with their intrinsic matrices  $I \in \mathbb{R}^{N_f \times 4 \times 4}$  and extrinsic matrices  $E \in \mathbb{R}^{N_f \times 4 \times 4}$ . We denote the projection of the 3D point cloud  $P$  on a frame with index  $i$   $P_i^{2D} \in \mathbb{R}^{4 \times N}$ , and it can be computed as follows  $P_i^{2D} = I_i \cdot E_i \cdot P$ . After stacking the projection operations of all frames, the projection of the scene onto all frames can be computed with a GPU in a single shot as follows

$$P^{2D} = (I \star E) \cdot P$$

where  $\star$  is batch-matrix multiplication,  $\cdot$  is matrix multiplication, and  $P^{2D} \in \mathbb{R}^{N_f \times 4 \times N}$  defined as  $P^{2D} = [P_1^{2D}, \dots, P_{N_f}^{2D}]$ .

Furthermore, we compute the visibility  $V^f \in \mathbb{Z}_2^{N_f \times N}$  of all projected points within all frames as follows

$$V^f = \mathbb{1}(0 < P_x^{2D} < W) \odot \mathbb{1}(0 < P_y^{2D} < H)$$

where  $\mathbb{1}$  is the indicator function,  $W$  and  $H$  are the image width and height respectively,  $\odot$  is element wise multiplication,  $P_x^{2D} \in \mathbb{R}^{N_f \times N}$  and  $P_y^{2D} \in \mathbb{R}^{N_f \times N}$  are the projected 3D points  $x$  and  $y$  coordinates on all  $N_f$  frames, respectively.

For occlusion, we define another visibility matrix as  $V^d \in \mathbb{Z}_2^{N_f \times N}$  that is computed as follows

$$V^d = \mathbb{1}(|P_z^{2D} - D_z| < \tau_{depth})$$

where  $D_z \in \mathbb{R}^{N_f \times N}$  is the real depth of the 3D point cloud obtained from the depth maps, while  $P_z^{2D} = P_{1 \leq i \leq N_f, j=3, 1 \leq k \leq N}^{2D}$  is the depth obtained from projecting the point cloud  $P$ , and  $|\cdot|$  is the absolute value. Finally, the per 3D mask proposal visibility  $\{V \in \mathbb{R}^{N_f \times K_{3D}}, 0 \leq V \leq 1\}$ , can be computed in a single shot using a GPU as follows

$$V = ((V^f \odot V^d) \cdot M^T) \odot M_{count}^{-1}$$

where  $M \in \mathbb{Z}_2^{K_{3D} \times N}$  is the matrix of 3D mask proposals generated by the 3D proposal network, and  $M_{count} \in \mathbb{N}^{K_{3D}}$  is the count of points per mask,

The percentage of visibility of a mask  $j$  in a frame  $i$  is represented with the element  $V_{i,j} \in V$ .

#### 4.5 Multi-View Prompt Distribution (MVPDist)

Given an RGB sequence  $\mathcal{I}$  and their corresponding LG label-maps  $\mathcal{L} = \{\mathcal{L}_i \mid \mathcal{L}_i \in \mathbb{Z}^{W \times H}, \forall i \in (1, \dots, K_f)\}$ . We define the label distribution  $\mathcal{D}_j \in \mathbb{Z}^{N_{dist}^j}$  of a 3D mask proposal  $M_j$  as

$$\mathcal{D}_j = \{\mathcal{L}_i [P_{i,x}^{2D} \cdot M_{ji}, P_{i,y}^{2D} \cdot M_{ji}] \mid \forall i \in \mathcal{P}_k\}$$

where  $M_{ji} = V_i^d \cdot V_i^f \cdot M_j$  is the mask for non-occluded in-frame points that belong to the  $j^{th}$  instance,  $\mathcal{P}_k$  is the set of frame indices where the  $j^{th}$  3D mask has top-k visibility, computed using the visibility matrix  $V$ ,  $P_{i,x}^{2D}$  and  $P_{i,y}^{2D}$  are the projected  $x$  and  $y$  coordinates of the point cloud scene

Table 1: **State-of-the-art comparison on ScanNet200 validation set.** We use Mask3D trained on the ScanNet200 training set to generate class-agnostic mask proposals. Our method demonstrates better performance compared to those that generate 3D proposals by fusing 2D masks and proposals from a 3D network (highlighted in gray in the table). It outperforms state-of-the-art methods by a wide margin under the same conditions using only proposals from a 3D network.

Method	3D proposals from 2D masks	SAM for 3D mask labeling	mAP	mAP50	mAP25	head	comm	tail	time/scene (s)
Mask3D [39] (Closed Vocab.)	×	×	26.9	36.2	41.4	39.8	21.7	17.9	13.41
SAM3D [50]	✓	×	6.1	14.2	21.3	7.0	6.2	4.6	482.60
OVIR-3D	✓	×	13.0	24.9	32.3	14.4	12.7	11.7	466.80
Open3DIS [34]	✓	×	23.7	29.4	32.8	27.8	21.2	21.8	360.12
OpenScene [35] (2D Fusion)	×	×	11.7	15.2	17.8	13.4	11.6	9.9	46.45
OpenScene [35] (3D Distill)	×	×	4.8	6.2	7.2	10.6	2.6	0.7	<b>0.26</b>
OpenScene [35] (2D-3D Ens.)	×	×	5.3	6.7	8.1	11.0	3.2	1.1	46.78
OpenMask3D [42]	×	✓	15.4	19.9	23.1	17.1	14.1	14.9	553.87
Open3DIS [34]	×	×	18.6	23.1	27.3	24.7	16.9	13.3	57.68
<b>Open-YOLO 3D (Ours)</b>	×	×	<b>24.7</b>	<b>31.7</b>	<b>36.2</b>	<b>27.8</b>	<b>24.3</b>	<b>21.6</b>	21.8

onto the  $i_{th}$  frame, respectively, while  $[\cdot, \cdot] : \mathbb{Z}^{W \times H} \mapsto \mathbb{Z}^n$  is a coordinate-based selection operator with  $n$  as an arbitrary natural number.

We define the probability for the mask  $M_j$  to be assigned to a class  $c$  as the occurrence of class  $c$  within the distribution  $\mathcal{D}_j$ ; we demonstrate the approach in Figure 3 for one 3D proposal. We assign the class with the highest probability to the mask  $M_j$ .

#### 4.6 Instance Prediction Confidence Score

We propose in this section a way to score class-agnostic 3D instance mask proposals by leveraging 2D information from bounding boxes along with 3D information from 3D masks. Our rationale is that a good mask should lead to a high class and mask confidence, unlike previous Open-Vocabulary 3D instance segmentation methods, which use only class confidence. To achieve this, we define the score of a 3D mask proposal as  $s_m = s_{IoU} \cdot s_{class}$ , where  $s_{class}$  is the probability of the class with the highest occurrence in MVPDist, while  $s_{IoU}$  is the average IoU across multi-views between the bounding box of the projected 3D mask and the bounding box with the highest IoU generated with a 2D object detector in the view (More details are in the appendix).

## 5 Experiments

**Datasets:** We conduct our experiments using the ScanNet200 [38] and Replica [40] datasets. Our analysis on ScanNet200 is based on its validation set, comprising 312 scenes. For the 3D instance segmentation task, we utilize the 200 predefined categories from the ScanNet200 annotations. ScanNet200 labels are categorized into three subsets—head (66 categories), common (68 categories), and tail (66 categories)—based on the frequency of labeled points in the training set. This categorization allows us to evaluate our method’s performance across the long-tail distribution, underscoring ScanNet200 as a suitable evaluation dataset. Additionally, to assess the generalizability of our approach, we conduct experiments on the Replica dataset, which has 48 categories. For the metrics, we follow the evaluation methodology in ScanNet [9] and report the average precision (AP) at two mask overlap thresholds: 50% and 25%, as well as the average across the overlap range of [0.5:0.95:0.05].

**Implementation details:** We use RGB-depth pairs from the ScanNet200 and Replica datasets, processing every 10th frame for ScanNet200 and all frames for Replica, maintaining the same settings as OpenMask3D for fair comparison. To create LG label maps, we use the YOLO-World [7] extra-large model for its real-time capability and high zero-shot performance. We use Mask3D [39] with non-maximum suppression to filter proposals similar to Open3DIS [34], and avoid DBSCAN [11] to prevent inference slowdowns. We use a single NVIDIA A100 40GB GPU for all experiments.

### 5.1 Results analysis

**Open-Vocabulary 3D instance segmentation on ScanNet200:** We compare our method’s performance against other approaches on the ScanNet200 dataset in Table 1. We indicate whether each

Table 2: **State-of-the-art comparison on Replica dataset.** We use Mask3D trained on the ScanNet200 training set to generate class-agnostic mask proposals. We show that our method generalizes better than state-of-the-art methods under the same setting with proposals from 3D networks only.

Method	3D proposals from 2D masks	SAM for 3D mask labeling	mAP	mAP50	mAP25	time/scene (s)
OVIR-3D	✓	×	11.1	20.5	27.5	52.74
Open3DIS [34]	✓	×	18.5	24.5	28.2	187.97
OpenScene [35] (2D fusion)	×	×	10.9	15.6	17.3	317.327
OpenScene [35] (3D Distill)	×	×	8.2	10.5	12.6	<b>04.29</b>
OpenScene [35] (2D-3D Ens.)	×	×	8.2	10.4	13.3	320.127
OpenMask3D [42]	×	✓	13.1	18.4	24.2	547.32
Open3DIS [34]	×	×	14.9	18.8	23.6	35.08
<b>Open-YOLO 3D (Ours)</b>	×	×	<b>23.7</b>	<b>28.6</b>	<b>34.8</b>	16.6

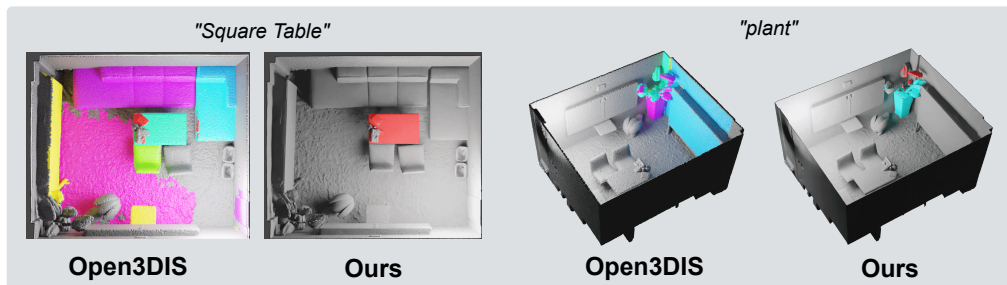


Figure 4: **Qualitative results on scene *office0* in the Replica dataset.** We show instances with a confidence score above 0.5 for both methods. We show that our method is much more precise when segmenting the object in the text compared to state-of-the-art method Open3DIS.

method uses 2D instances to generate 3D proposals and whether SAM is used for labeling the 3D masks. Our method achieves state-of-the-art performance with proposals from only a 3D instance segmentation network compared to methods from two settings (*i*) 3D mask proposals from only a 3D instance segmentation network (*ii*) using a combination of 3D mask proposals from a 3D network and 2D instances from a 2D segmentation model. Additionally, our method is  $\sim 16\times$  faster compared to state-of-the-art Open3DIS.

**Generalizability test:** To test the generalizability of our method, we use the 3D proposal network pre-trained on the ScanNet200 training set and evaluate on the Replica dataset; the results are shown in Table 2. Our method shows competitive performance with  $\sim 11 \times$  speedup against state-of-the-art models [34], which use CLIP features.

**Performance with given 3D masks:** We further test our method for 3D proposal prompting from text against existing methods in the literature in the case of ground truth 3D masks and report the results in Table 5. For Mask3D, oracle masks are assigned class predictions from matched predicted masks using Hungarian matching. For open-vocabulary methods, we use ground-truth masks as input proposals. We show the results in Table 5 that MVPDist can out-

perform CLIP-based approaches in retrieving the correct 3D proposal masks from text prompts, due to the high zero-shot performance achieved by state-of-the-art open-vocabulary 2D object detectors.

Method	2D OV Prior	mAP	head	comm	tail
<i>Closed Vocab.</i>					
Mask3D [39]	None	35.5	55.2	27.2	22.2
OpenScene [35]	2D LSeg [27]	11.8	26.9	5.2	1.7
OpenScene [35]	2D OpenSeg [12]	22.9	26.2	22.0	20.2
OpenMask3D [42]	Mask wise CLIP [37]	29.1	31.1	24.0	32.9
Open3DIS [34]	Point wise CLIP [37]	30.9	33.1	25.1	35.4
<b>Open-YOLO 3D (Ours)</b>	MVPDist	<b>39.6</b>	<b>43.3</b>	<b>36.8</b>	<b>38.5</b>

perform CLIP-based approaches in retrieving the correct 3D proposal masks from text prompts, due to the high zero-shot performance achieved by state-of-the-art open-vocabulary 2D object detectors.

Table 3: **Ablation study on Replica dataset with ground truth masks.** We show the effect of replacing SAM with a 2D object detector in rows R2 to R4 while we demonstrate the effect of replacing CLIP features with MVPDist with label maps from an OV 2D object detector.

Row ID ↓	2D Prior	Labeling method	MVPDist	VAcc	mAP	time/scene (s)
R1	SAM[23]+CLIP	Clip features	×	×	33.0	675.6
R2	YoloV8+CLIP	Clip features	×	×	21.1	440.40
R3	RT-DETR[57]+CLIP	Clip features	×	×	28.4	487.95
R4	YoloWorld[7]+CLIP	Clip features	×	×	32.5	384.29
R5	YoloWorld	LG Label Maps	✓	×	46.2	376.42
R6	YoloWorld	LG Label Maps	✓	✓	<b>46.2</b>	<b>17.86</b>

Table 4: **Effect of number of top-k views on the labeling performance with High Granularity (HG) and Low-Granularity (LG) label maps.** HG Label maps are generated by prompting SAM with the bounding boxes used to generate LG label maps.

Topk (→)	1	10	20	30	40
Map type (↓)	mAP/ time(s)	mAP/ time(s)	mAP/ time(s)	mAP/ time(s)	mAP/ time(s)
HG label maps	16.3/113.93	22.5 / 115.16	23.9 / 114.76	24.4 / 115.89	24.5 / 115.92
LG label maps	16.3 / 20.7	22.8 / 21.6	24.3 / 21.7	24.6 / 22.1	24.7 / 22.2

**Ablation over Replica dataset:** To test the ability of object detectors to replace SAM for generating crops for 3D CLIP feature aggregation, we conduct three experiments with different object detectors on the Replica dataset, using ground truth 3D mask proposals to compare our method’s labeling ability against others. The results are in Table 3, rows **R2** to **R4**, with row **R1** showing OpenMask3D [42] base code results. We generate class-agnostic bounding boxes with an object detector, then assign the highest IoU bounding box to each 3D instance as a crop, selecting the most visible views. For 3D CLIP feature aggregation, we follow OpenMask3D’s approach, aggregating features from multiple levels and views. These experiments show that YOLO-World can generate crops nearly as good as SAM but with significant speed improvements. Row **R5** demonstrates YOLO-World’s better zero-shot performance using our proposed Multi-View Prompt Distribution with LG label maps. Row **R6** shows speed improvements using the GPU for 3D mask visibility computation.

**Top K analysis:** We show in Table 4 that naively using YOLO-World with only one label-map with the highest visibility per 3D mask proposal results in sub-optimal results and using top-K label-maps can result in better predictions as the distribution can provide better estimate across multiple frames, since YOLO-World is also expected to make misclassifications in some views while generating correct ones in others. This approach assumes that YOLO-World makes a correct class prediction for the same 3D object in multiple views for it to be effective.

**High-Granularity (HG) vs. Low-Granularity (LG):** Table 4 shows that using SAM to generate HG label maps slightly reduces mAP, and slows down the inference by  $\sim 5$  times. This is due to the nature of projected 3D instances into 2D, where the projection already holds 2D instance information as shown in Figure 3, and SAM would just result in redundancy in the prediction.

**Qualitative results:** We show qualitative results on the Replica dataset in Figure 4 and compare it to Open3DIS. Open3DIS shows good performance in recalling novel geometries that 3D proposal networks like Mask3D generally fail to capture (small-sized objects). However, it comes at the cost of very low precision due to the redundant masks with different class predictions.

**Limitations:** Our method makes use of a 3D proposal network only for proposal generation in order to reach high speed. Other proposal generation methods [32, 34] fuse 2D instance masks from a 2D instance segmentation methods to generate rich 3D proposals even for very small objects, which are generally overlooked by 3D proposal networks like Mask3D [39] due to low resolution in 3D. Thus, fast 2D instance segmentation models like FastSAM [56] can be used to generate 3D proposals from the 2D images, which might further improve the performance of our method.

## 6 Conclusion

We present Open-YOLO 3D, a novel and efficient open-vocabulary 3D instance segmentation method, which makes use of open-vocabulary 2D object detectors instead of heavy segmentation models. Our approach leverages a 2D object detector for class-labeled bounding boxes and a 3D instance segmentation network for class-agnostic masks. We propose to use MVPDist generated from multi-view low granularity label maps to match text prompts to 3D class agnostic masks. Our proposed method outperforms existing techniques, with gains in mAP and inference speed. These results show a new direction toward more efficient open-vocabulary 3D instance segmentation models.

## References

- [1] S. Al Khatib, M. El Amine Boudjoghra, J. Lahoud, and F. S. Khan. 3d instance segmentation via enhanced spatial and semantic supervision. In *Proceedings of the IEEE/CVF International Conference on Computer Vision*, pages 541–550, 2023.
- [2] M. E. A. Boudjoghra, S. K. A. Khatib, J. Lahoud, H. Cholakkal, R. M. Anwer, S. Khan, and F. Khan. 3d indoor instance segmentation in an open-world. In *Advances in Neural Information Processing Systems*, 2023.
- [3] M. Bucher, T.-H. Vu, M. Cord, and P. Pérez. Zero-shot semantic segmentation. *Advances in Neural Information Processing Systems*, 32, 2019.
- [4] S. Chen, J. Fang, Q. Zhang, W. Liu, and X. Wang. Hierarchical aggregation for 3d instance segmentation. In *Proceedings of the IEEE/CVF International Conference on Computer Vision*, pages 15467–15476, 2021.
- [5] B. Cheng, I. Misra, A. G. Schwing, A. Kirillov, and R. Girdhar. Masked-attention mask transformer for universal image segmentation. In *Proceedings of the IEEE/CVF Conference on Computer Vision and Pattern Recognition*, pages 1290–1299, 2022.
- [6] B. Cheng, A. Schwing, and A. Kirillov. Per-pixel classification is not all you need for semantic segmentation. *Advances in Neural Information Processing Systems*, 34:17864–17875, 2021.
- [7] T. Cheng, L. Song, Y. Ge, W. Liu, X. Wang, and Y. Shan. Yolo-world: Real-time open-vocabulary object detection. In *Proc. IEEE Conf. Computer Vision and Pattern Recognition (CVPR)*, 2024.
- [8] J. Chibane, F. Engelmann, T. Anh Tran, and G. Pons-Moll. Box2mask: Weakly supervised 3d semantic instance segmentation using bounding boxes. In *Computer Vision—ECCV 2022: 17th European Conference, Tel Aviv, Israel, October 23–27, 2022, Proceedings, Part XXXI*, pages 681–699. Springer, 2022.
- [9] A. Dai, A. X. Chang, M. Savva, M. Halber, T. Funkhouser, and M. Nießner. Scannet: Richly-annotated 3d reconstructions of indoor scenes. In *Proc. Computer Vision and Pattern Recognition (CVPR)*, IEEE, 2017.
- [10] F. Engelmann, M. Bokeloh, A. Fathi, B. Leibe, and M. Nießner. 3d-mpa: Multi-proposal aggregation for 3d semantic instance segmentation. In *Proceedings of the IEEE/CVF conference on computer vision and pattern recognition*, pages 9031–9040, 2020.
- [11] M. Ester, H.-P. Kriegel, J. Sander, and X. Xu. A density-based algorithm for discovering clusters in large spatial databases with noise. In *Proceedings of the Second International Conference on Knowledge Discovery and Data Mining, KDD’96*, page 226–231. AAAI Press, 1996.
- [12] G. Ghiasi, X. Gu, Y. Cui, and T.-Y. Lin. Scaling open-vocabulary image segmentation with image-level labels. In *European Conference on Computer Vision*, pages 540–557. Springer, 2022.
- [13] Q. Gu, A. Kuwajerwala, K. M. Jatavallabhula, B. Sen, A. Agarwal, C. Rivera, W. Paul, R. Chellappa, C. Gan, C. M. de Melo, et al. Conceptgraphs: Open-vocabulary 3d scene graphs for perception and planning. In *2nd Workshop on Language and Robot Learning: Language as Grounding*, 2023.
- [14] L. Han, T. Zheng, L. Xu, and L. Fang. Occuseg: Occupancy-aware 3d instance segmentation. In *Proceedings of the IEEE/CVF conference on computer vision and pattern recognition*, pages 2940–2949, 2020.

- [15] T. He, C. Shen, and A. Van Den Hengel. Dyc3d: Robust instance segmentation of 3d point clouds through dynamic convolution. In *Proceedings of the IEEE/CVF conference on computer vision and pattern recognition*, pages 354–363, 2021.
- [16] Y. Hong, C. Lin, Y. Du, Z. Chen, J. B. Tenenbaum, and C. Gan. 3d concept learning and reasoning from multi-view images. In *Proceedings of the IEEE/CVF Conference on Computer Vision and Pattern Recognition*, pages 9202–9212, 2023.
- [17] J. Hou, A. Dai, and M. Nießner. 3d-sis: 3d semantic instance segmentation of rgb-d scans. In *Proceedings of the IEEE/CVF conference on computer vision and pattern recognition*, pages 4421–4430, 2019.
- [18] J. Hou, B. Graham, M. Nießner, and S. Xie. Exploring data-efficient 3d scene understanding with contrastive scene contexts. In *Proceedings of the IEEE/CVF Conference on Computer Vision and Pattern Recognition*, pages 15587–15597, 2021.
- [19] D. Huynh, J. Kuen, Z. Lin, J. Gu, and E. Elhamifar. Open-vocabulary instance segmentation via robust cross-modal pseudo-labeling. In *Proceedings of the IEEE/CVF Conference on Computer Vision and Pattern Recognition*, pages 7020–7031, 2022.
- [20] A. Jain, P. Katara, N. Gkanatsios, A. W. Harley, G. Sarch, K. Aggarwal, V. Chaudhary, and K. Fragkiadaki. Odin: A single model for 2d and 3d perception. In *Proceedings of the IEEE/CVF Conference on Computer Vision and Pattern Recognition*, 2024.
- [21] L. Jiang, H. Zhao, S. Shi, S. Liu, C.-W. Fu, and J. Jia. Pointgroup: Dual-set point grouping for 3d instance segmentation. In *Proceedings of the IEEE/CVF conference on computer vision and Pattern recognition*, pages 4867–4876, 2020.
- [22] P. Kaul, W. Xie, and A. Zisserman. Multi-modal classifiers for open-vocabulary object detection. In *International Conference on Machine Learning*, 2023.
- [23] A. Kirillov, E. Mintun, N. Ravi, H. Mao, C. Rolland, L. Gustafson, T. Xiao, S. Whitehead, A. C. Berg, W.-Y. Lo, et al. Segment anything. In *Proceedings of the IEEE/CVF International Conference on Computer Vision*, pages 4015–4026, 2023.
- [24] M. Kolodiazhyi, A. Vorontsova, A. Konushin, and D. Rukhovich. Oneformer3d: One transformer for unified point cloud segmentation. In *Proceedings of the IEEE/CVF Conference on Computer Vision and Pattern Recognition*, 2024.
- [25] J. Lahoud, J. Cao, F. S. Khan, H. Cholakkal, R. M. Anwer, S. Khan, and M.-H. Yang. 3d vision with transformers: A survey, 2022.
- [26] J. Lahoud, B. Ghanem, M. Pollefeys, and M. R. Oswald. 3d instance segmentation via multi-task metric learning. In *Proceedings of the IEEE/CVF International Conference on Computer Vision*, pages 9256–9266, 2019.
- [27] B. Li, K. Q. Weinberger, S. Belongie, V. Koltun, and R. Ranftl. Language-driven semantic segmentation. In *International Conference on Learning Representations*, 2021.
- [28] F. Liang, B. Wu, X. Dai, K. Li, Y. Zhao, H. Zhang, P. Zhang, P. Vajda, and D. Marculescu. Open-vocabulary semantic segmentation with mask-adapted clip. In *Proceedings of the IEEE/CVF Conference on Computer Vision and Pattern Recognition*, pages 7061–7070, 2023.
- [29] Z. Liang, Z. Li, S. Xu, M. Tan, and K. Jia. Instance segmentation in 3d scenes using semantic superpoint tree networks. In *Proceedings of the IEEE/CVF International Conference on Computer Vision*, pages 2783–2792, 2021.
- [30] S. Liu, Z. Zeng, T. Ren, F. Li, H. Zhang, J. Yang, C. Li, J. Yang, H. Su, J. Zhu, et al. Grounding dino: Marrying dino with grounded pre-training for open-set object detection. *arXiv preprint arXiv:2303.05499*, 2023.
- [31] S.-H. Liu, S.-Y. Yu, S.-C. Wu, H.-T. Chen, and T.-L. Liu. Learning gaussian instance segmentation in point clouds. *arXiv preprint arXiv:2007.09860*, 2020.
- [32] S. Lu, H. Chang, E. P. Jing, A. Boularias, and K. Bekris. Ovir-3d: Open-vocabulary 3d instance retrieval without training on 3d data. In *Conference on Robot Learning*, pages 1610–1620. PMLR, 2023.
- [33] C. Ma, Y. Yuhuan, C. Ju, F. Zhang, Y. Zhang, and Y. Wang. Open-vocabulary semantic segmentation via attribute decomposition-aggregation. *Advances in Neural Information Processing Systems*, 36, 2024.

- [34] P. D. Nguyen, T. D. Ngo, C. Gan, E. Kalogerakis, A. Tran, C. Pham, and K. Nguyen. Open3dis: Open-vocabulary 3d instance segmentation with 2d mask guidance. In *Proceedings of the IEEE/CVF Conference on Computer Vision and Pattern Recognition*, 2024.
- [35] S. Peng, K. Genova, C. Jiang, A. Tagliasacchi, M. Pollefeys, T. Funkhouser, et al. Openscene: 3d scene understanding with open vocabularies. In *Proceedings of the IEEE/CVF Conference on Computer Vision and Pattern Recognition*, pages 815–824, 2023.
- [36] C. Pham, T. Vu, and K. Nguyen. Lp-ovod: Open-vocabulary object detection by linear probing. In *Proceedings of the IEEE/CVF Winter Conference on Applications of Computer Vision*, pages 779–788, 2024.
- [37] A. Radford, J. W. Kim, C. Hallacy, A. Ramesh, G. Goh, S. Agarwal, G. Sastry, A. Askell, P. Mishkin, J. Clark, et al. Learning transferable visual models from natural language supervision. In *International conference on machine learning*, pages 8748–8763. PMLR, 2021.
- [38] D. Rozenberszki, O. Litany, and A. Dai. Language-grounded indoor 3d semantic segmentation in the wild. In *Proceedings of the European Conference on Computer Vision (ECCV)*, 2022.
- [39] J. Schult, F. Engelmann, A. Hermans, O. Litany, S. Tang, and B. Leibe. Mask3D: Mask Transformer for 3D Semantic Instance Segmentation. In *International Conference on Robotics and Automation (ICRA)*, 2023.
- [40] J. Straub, T. Whelan, L. Ma, Y. Chen, E. Wijmans, S. Green, J. J. Engel, R. Mur-Artal, C. Ren, S. Verma, A. Clarkson, M. Yan, B. Budge, Y. Yan, X. Pan, J. Yon, Y. Zou, K. Leon, N. Carter, J. Briales, T. Gillingham, E. Mueggler, L. Pesqueira, M. Savva, D. Batra, H. M. Strasdat, R. D. Nardi, M. Goesele, S. Lovegrove, and R. Newcombe. The replica dataset: A digital replica of indoor spaces, 2019.
- [41] J. Sun, C. Qing, J. Tan, and X. Xu. Superpoint transformer for 3d scene instance segmentation. In *Proceedings of the AAAI Conference on Artificial Intelligence*, 2023.
- [42] A. Takmaz, E. Fedele, R. Sumner, M. Pollefeys, F. Tombari, and F. Engelmann. Openmask3d: Open-vocabulary 3d instance segmentation. *Advances in Neural Information Processing Systems*, 36, 2023.
- [43] A. Vaswani, N. Shazeer, N. Parmar, J. Uszkoreit, L. Jones, A. N. Gomez, Ł. Kaiser, and I. Polosukhin. Attention is all you need. *Advances in neural information processing systems*, 30, 2017.
- [44] V. VS, N. Yu, C. Xing, C. Qin, M. Gao, J. C. Niebles, V. M. Patel, and R. Xu. Mask-free ovis: Open-vocabulary instance segmentation without manual mask annotations. In *Proceedings of the IEEE/CVF Conference on Computer Vision and Pattern Recognition*, pages 23539–23549, 2023.
- [45] L. Wang, Y. Liu, P. Du, Z. Ding, Y. Liao, Q. Qi, B. Chen, and S. Liu. Object-aware distillation pyramid for open-vocabulary object detection. In *Proceedings of the IEEE/CVF Conference on Computer Vision and Pattern Recognition*, pages 11186–11196, 2023.
- [46] W. Wang, R. Yu, Q. Huang, and U. Neumann. Sgpn: Similarity group proposal network for 3d point cloud instance segmentation. In *Proceedings of the IEEE conference on computer vision and pattern recognition*, pages 2569–2578, 2018.
- [47] S. Xie, J. Gu, D. Guo, C. R. Qi, L. Guibas, and O. Litany. Pointcontrast: Unsupervised pre-training for 3d point cloud understanding. In *Computer Vision—ECCV 2020: 16th European Conference, Glasgow, UK, August 23–28, 2020, Proceedings, Part III 16*, pages 574–591. Springer, 2020.
- [48] J. Xu, S. De Mello, S. Liu, W. Byeon, T. Breuel, J. Kautz, and X. Wang. Groupvit: Semantic segmentation emerges from text supervision. In *Proceedings of the IEEE/CVF Conference on Computer Vision and Pattern Recognition*, pages 18134–18144, 2022.
- [49] B. Yang, J. Wang, R. Clark, Q. Hu, S. Wang, A. Markham, and N. Trigoni. Learning object bounding boxes for 3d instance segmentation on point clouds. *Advances in neural information processing systems*, 32, 2019.
- [50] Y. Yang, X. Wu, T. He, H. Zhao, and X. Liu. Sam3d: Segment anything in 3d scenes, 2023.
- [51] L. Yao, J. Han, X. Liang, D. Xu, W. Zhang, Z. Li, and H. Xu. Detclipv2: Scalable open-vocabulary object detection pre-training via word-region alignment. In *Proceedings of the*

- IEEE/CVF Conference on Computer Vision and Pattern Recognition*, pages 23497–23506, 2023.
- [52] L. Yi, W. Zhao, H. Wang, M. Sung, and L. J. Guibas. Gspn: Generative shape proposal network for 3d instance segmentation in point cloud. In *Proceedings of the IEEE/CVF Conference on Computer Vision and Pattern Recognition*, pages 3947–3956, 2019.
  - [53] Y. Zang, W. Li, K. Zhou, C. Huang, and C. C. Loy. Open-vocabulary detr with conditional matching. In *European Conference on Computer Vision*, pages 106–122. Springer, 2022.
  - [54] B. Zhang and P. Wonka. Point cloud instance segmentation using probabilistic embeddings. In *Proceedings of the IEEE/CVF Conference on Computer Vision and Pattern Recognition*, pages 8883–8892, 2021.
  - [55] J. Zhang, R. Dong, and K. Ma. Clip-fo3d: Learning free open-world 3d scene representations from 2d dense clip. In *Proceedings of the IEEE/CVF International Conference on Computer Vision*, pages 2048–2059, 2023.
  - [56] X. Zhao, W. Ding, Y. An, Y. Du, T. Yu, M. Li, M. Tang, and J. Wang. Fast segment anything. *arXiv preprint arXiv:2306.12156*, 2023.
  - [57] Y. Zhao, W. Lv, S. Xu, J. Wei, G. Wang, Q. Dang, Y. Liu, and J. Chen. Detsr beat yolos on real-time object detection. In *Proceedings of the IEEE/CVF Conference on Computer Vision and Pattern Recognition (CVPR)*, 2024.
  - [58] Y. Zhong, J. Yang, P. Zhang, C. Li, N. Codella, L. H. Li, L. Zhou, X. Dai, L. Yuan, Y. Li, et al. Regionclip: Region-based language-image pretraining. In *Proceedings of the IEEE/CVF Conference on Computer Vision and Pattern Recognition*, pages 16793–16803, 2022.

## A Appendix

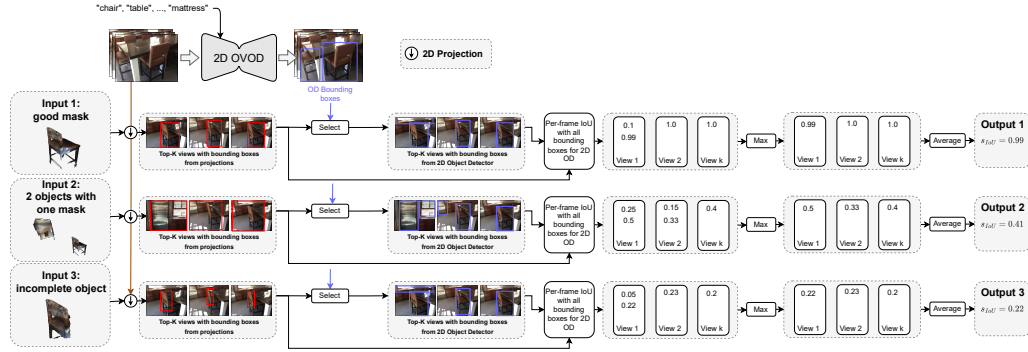


Figure 5: **Additional details on how IoU score  $s_{IoU}$  is computed.** We show that our method can provide a reliable mask score using Intersection Over Union (IoU) between the bounding boxes estimated using the 3D cropped instance 2D projection and the bounding boxes from a 2D object detector. We also demonstrate that it covers all three cases of different 3D mask proposals.

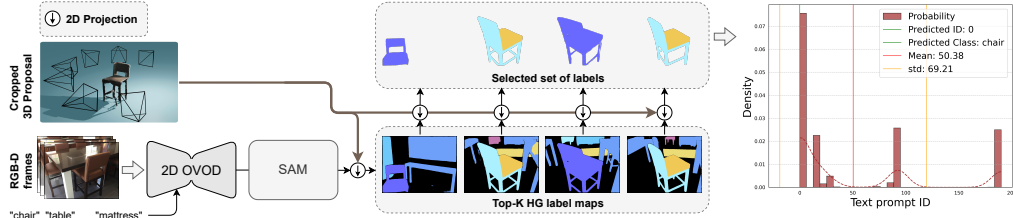


Figure 6: **Additional details on how the High-Granularity label maps (HG label maps) are constructed.** To get a detailed per-pixel label for the label maps, we prompt SAM with bounding boxes to get pixel-wise masks, and then we follow the same approach as in Section 4.3 to construct the label maps. The multi-View Prompt Distribution is estimated in the same way as in Section 4.5

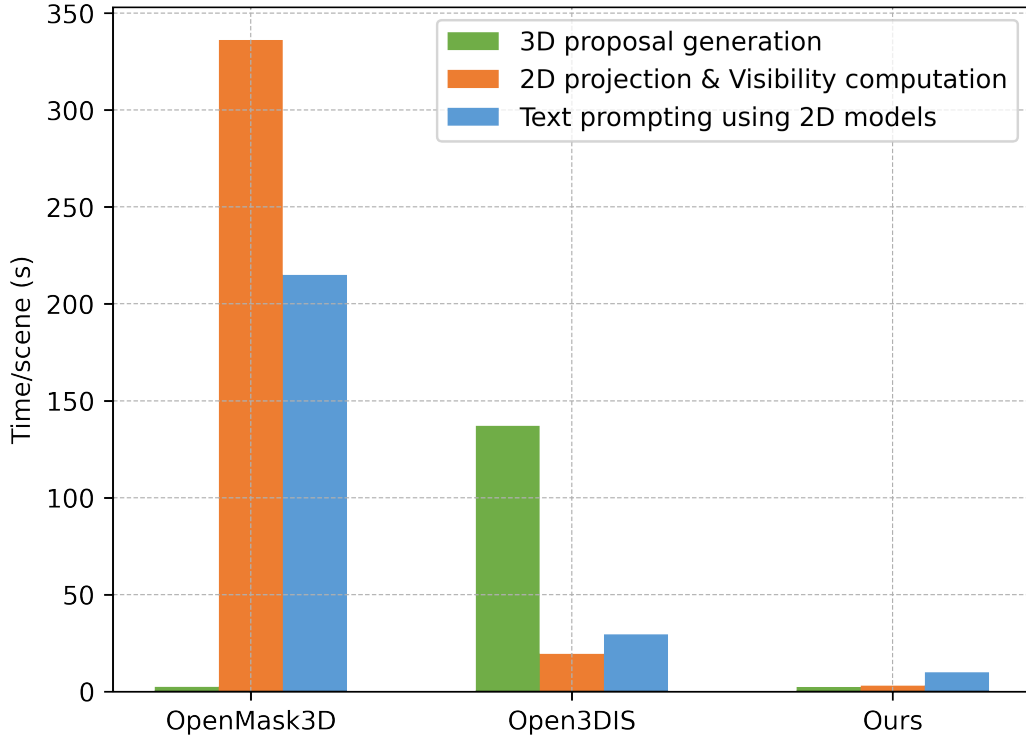


Figure 7: **Time breakdown of the average time for Open-Vocabulary 3D instance segmentation over the replica dataset.** We report the time for each step that makes the whole Open-Vocabulary 3D instance segmentation pipeline for our method and the two most recent methods, OpenMask3D and Open3DIS. **3D proposal generation** is the step of generating class agnostic mask proposals for the objects in the 3D point cloud scene **2D projection & Visibility computation** is the step of projection of the point cloud scene onto the 2D frames, and computing the visibility of each mask proposal in the 2D frames. **Text prompting with 2D models** is the step of inference from the 2D models to prompt the 3D class agnostic masks with text.

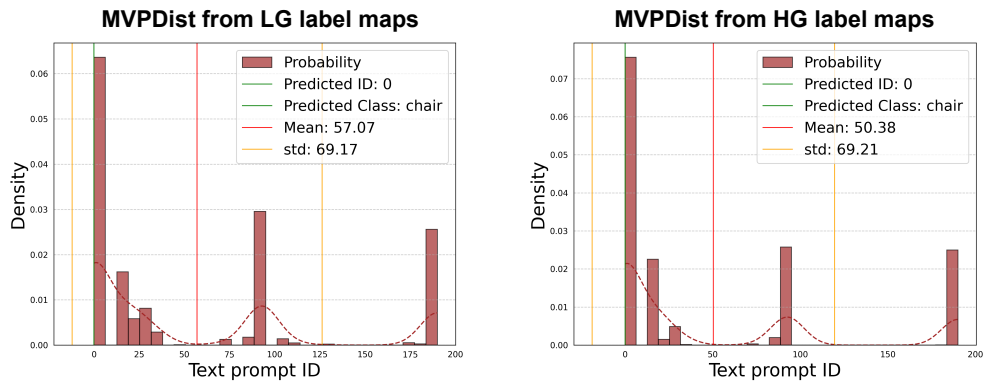


Figure 8: **Comparison between MVPDist with HG label maps and with LG label maps.** We show that using HG label maps instead of LG label maps slightly increases the prediction class score but results in the same prediction. Thus, LG can give a similar performance with around 5 times speed up in terms of inference time.

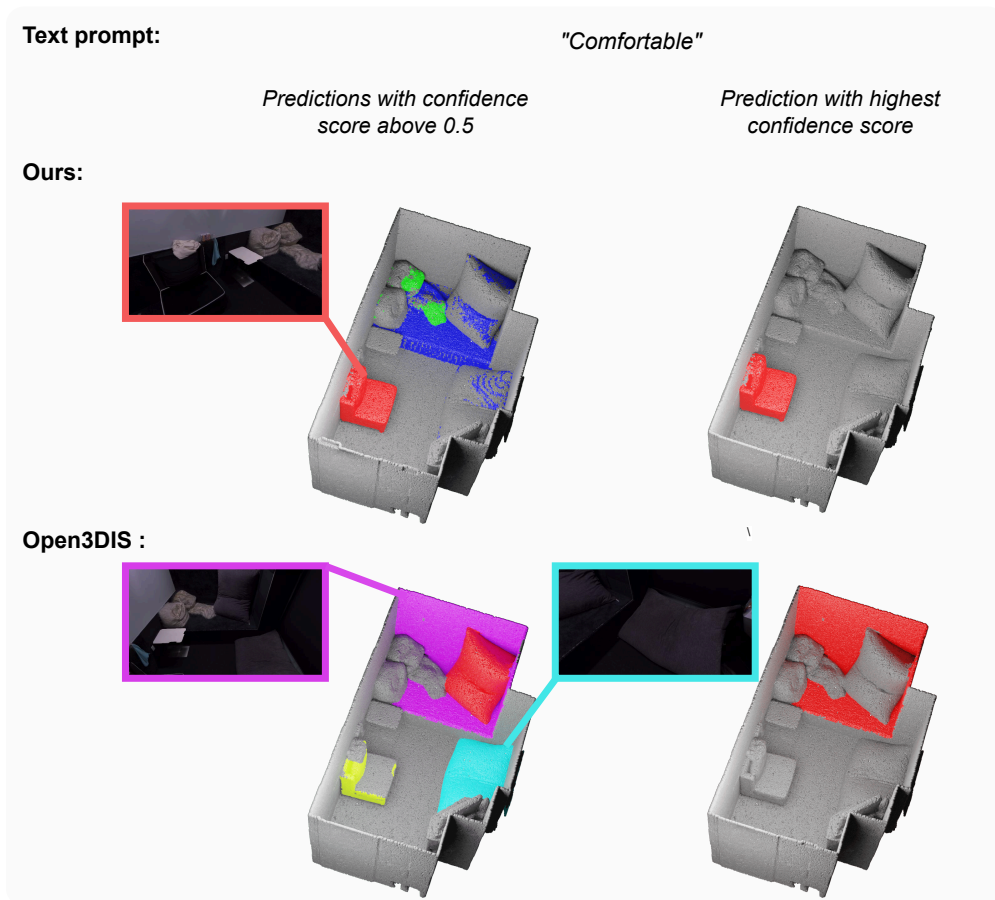


Figure 9: **Comparison between our method and Open3DIS.** We show that our method is more precise than Open3DIS.

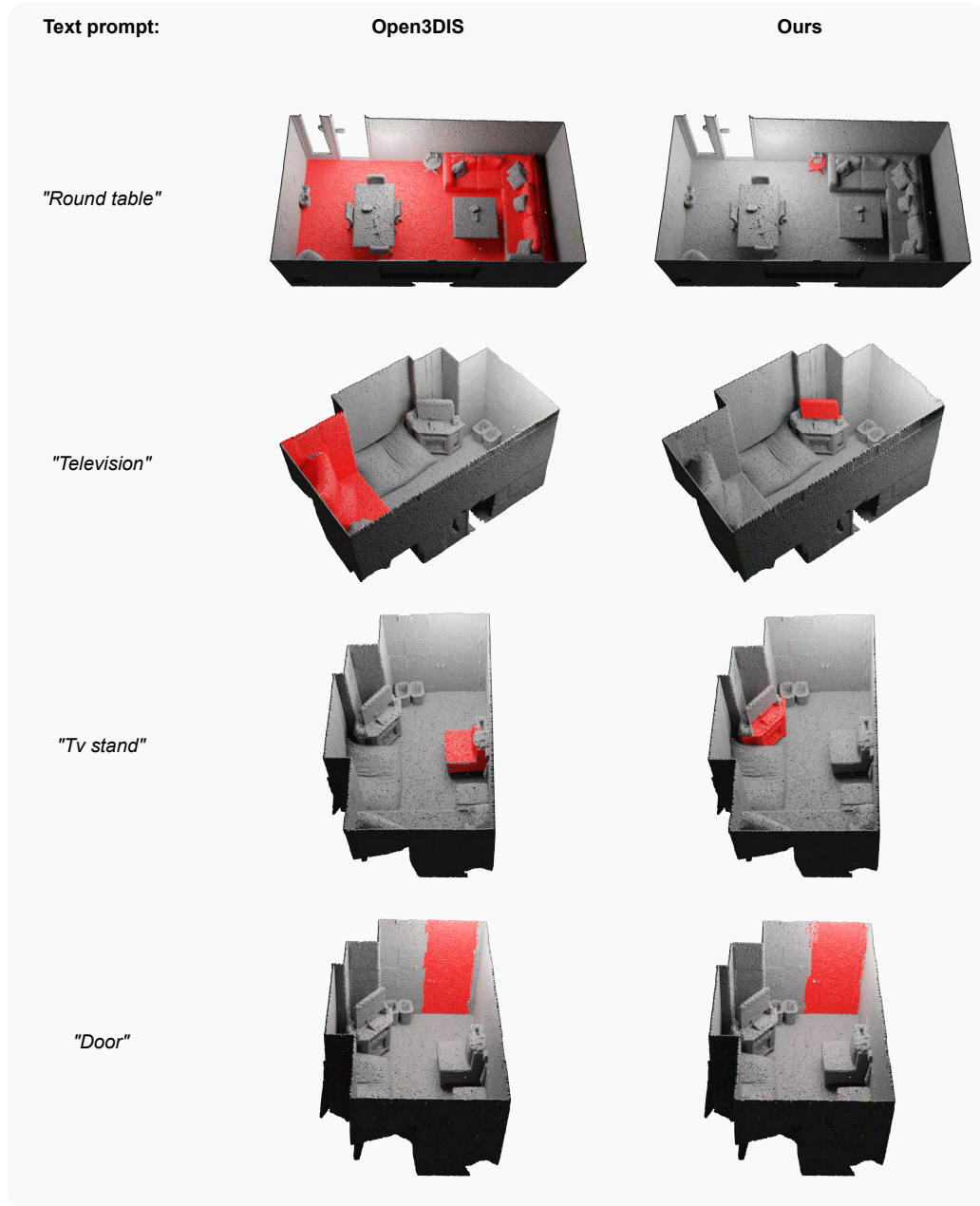


Figure 10: Comparison of prediction with the highest score between our method and Open3DIS on replica dataset.

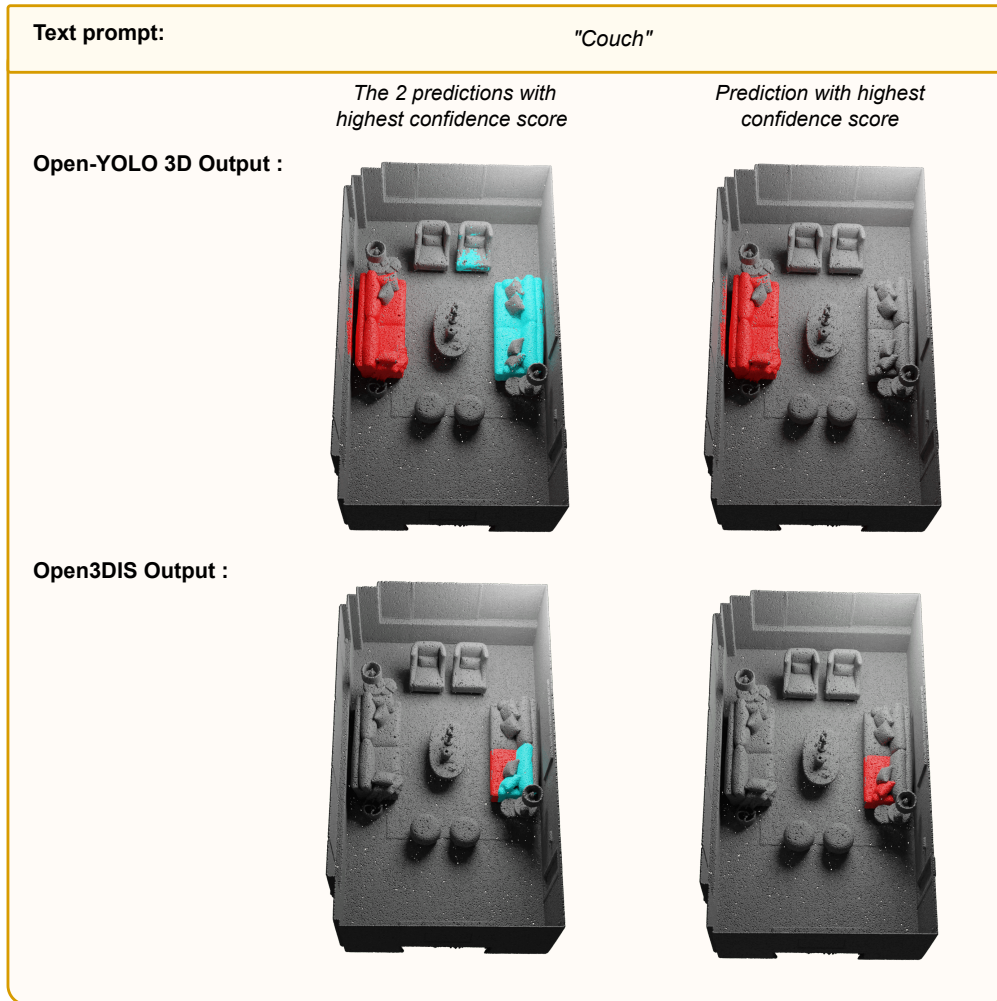


Figure 11: **Scoring quality comparison between ours and Open3DIS.** (Top) We show on the left the two masks with top confidence scores  $s_m$  computed as in section 4.6, notice that the second mask in blue has a portion that extends to another instance, which makes it worse in than the red mask. Our scoring technique captures this detail while scoring the mask. (Bottom) We show on the left the two masks with the highest scores by Open3DIS. Notice that using only semantic scores results in wrong mask confidence since it is aggregated from 2D clip features, where points with the most visibility across views contribute more than others to the final aggregated 3D clip features. Thus, this type of scoring assigns very high scores to bad masks that have points with more visibility.



Figure 12: **Additional qualitative results on ScanNet200.** with text prompt *"Chair"*.



Figure 13: **Additional qualitative results on ScanNet200.** with text prompt *"Table"*.

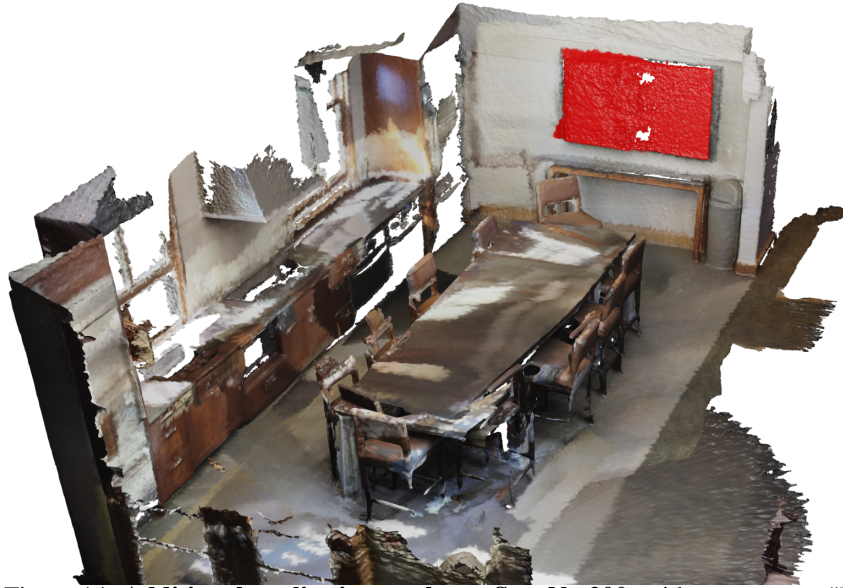


Figure 14: Additional qualitative results on ScanNet200. with text prompt *"Television"*.

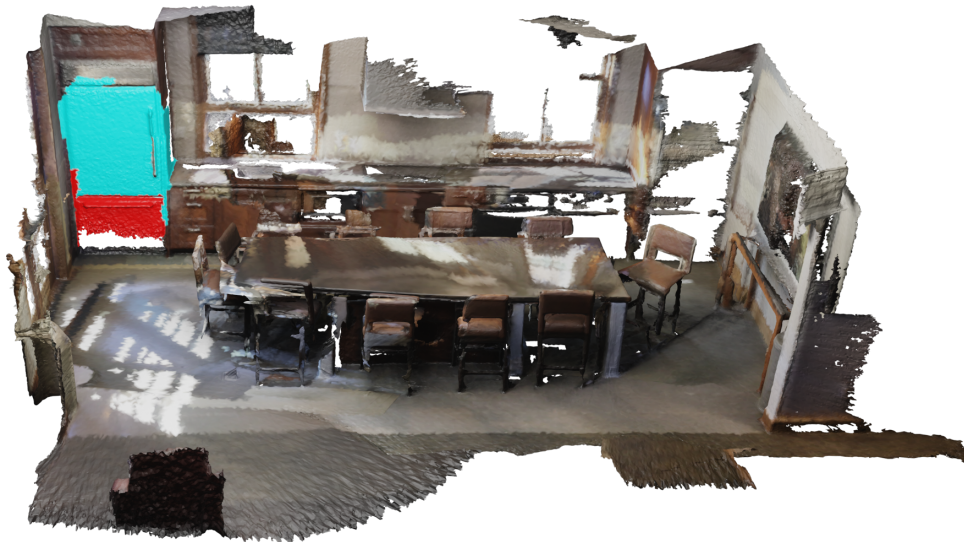


Figure 15: Additional qualitative results on ScanNet200. with text prompt *"Fridge"*.

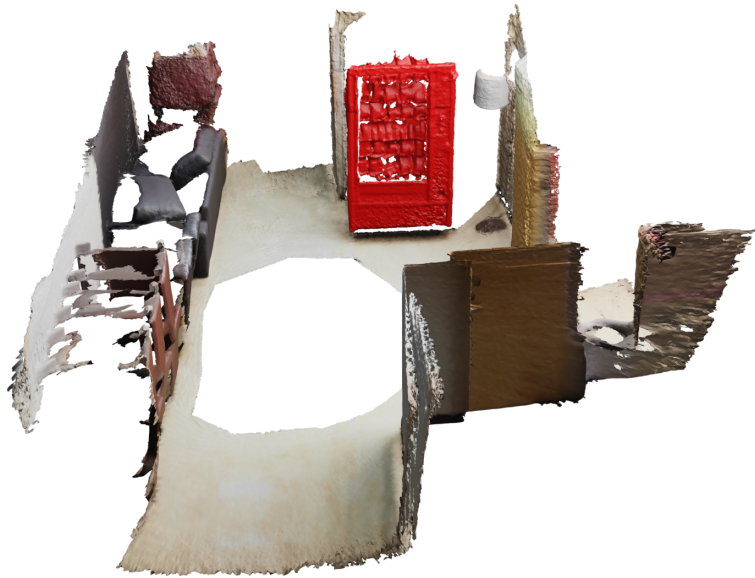


Figure 16: **Additional qualitative results on ScanNet200.** with text prompt *"Snacks"*.



Figure 17: **Additional qualitative results on ScanNet200.** with text prompt *"Computer"*.



Figure 18: Additional qualitative results on ScanNet200. with text prompt *"Desk"*.



Figure 19: Additional qualitative results on ScanNet200. with text prompt *"Bed"*.



Figure 20: **Additional qualitative results on ScanNet200.** with text prompt "*Shoes*".